Electrical transport properties of semimetallic GdX single crystals (X=P, As, Sb, and Bi)

D. X. Li,* Y. Haga, H. Shida, and T. Suzuki
Department of Physics, Tohoku University, Sendai 980-77, Japan

Y. S. Kwon
Department of Physics, Suny Kyun Kwan University, Suwon, South Korea

(Received 26 April 1996)

The large single crystals of stoichiometric and nonstoichiometric Gd monopnictides GdX (X=P, As, Sb, and Bi) are grown by the mineralization method (for X=P and As) and Bridgman method (for X=Sb and Bi). A systematic investigation of the transport properties of GdX single crystals is presented. We report on measurements of the electric resistivity $\rho(T)$, magnetoresistance $\rho(H)$, and Hall effect performed on the stoichiometric and nonstoichiometric samples at temperatures between 1.6 and 300 K in magnetic fields up to 10 T. The stoichiometric samples behaved as the well-compensated semimetals that order antiferromagnetically at Néel temperatures T_N=15.9 K for GdP, 18.7 K for GdAs, 23.4 K for GdSb, and 25.8 K for GdBi. The transverse magnetoresistance measured at low temperature follows a $\rho(H) \propto H^2$ law, and a larger positive ratio MRR $=[\rho(H)-\rho(0)]/\rho(0)$ is observed at 10 T for the four stoichiometric samples. The temperature dependence of the resistivity can be explained by the $d-f$ Coulomb exchange interaction at lower temperatures. The Hall-effect measurements yield a carrier concentration $n=2.1\times10^{20}$ cm^{-3} for GdAs and $n=4.2\times10^{20}$ cm^{-3} for GdSb, which are in a good agreement with the de Haas–van Alphen effect measurements. The nonstoichiometric samples showed some anomalies that could be explained qualitatively by the model of trapped magnetic polaron. [S0163-1829(96)00239-1]

I. INTRODUCTION

Anomalous physical properties observed in the rare-earth monopnictides RX (X=N, P, As, Sb, and Bi) have attracted much attention in recent years,[1–3] because they are the typical low carrier strongly correlated systems with simple rocksalt crystal structure. In the rare-earth monopnictides, the conduction band is formed by the $5d$ orbitals of the cation R and has its minimum at the X point of the Brilloun zone, while the valence band formed mainly by the anionic np state of X (n=2, 3, 4, 5, and 6 for X=N, P, As, Sb, and Bi, respectively) has its maximum at the center of the Brilloun zone. A weak overlap between the bottom of the conduction band and the top of the valence band is sufficient to make semimetals with a low carrier concentration out of these materials.[4,5] In most cases, the direct exchange interaction between $4f$ ions in RX systems is weak due to the majority of $4f$ electrons that lie well inside the $5s$ and $5p$ closed shells and are well screened by them. Thus, the indirect exchange interaction between $4f$ ions must be the main mechanism, and charge carriers act as the intermediary of this indirect exchange interaction. In the various RX compounds, the indirect exchange interaction leads to different magnetic and transport properties, depending on the free-carrier concentration (the overlap between valence band and conduction band), the position of $4f$ level as well as its splitting form in crystalline electric field (CEF). Among the RX systems, Gd monopnictides are the most simple series, because Gd is located in the center of the series of the rare-earth metals in the Periodic Table of the elements, the Gd^{3+} ion appearing in GdX has a $4f^7$ configuration and is an S-state ion with spin $\frac{7}{2}$ and no orbital momentum, the CEF effects in GdX are considered to be fairly weak. Furthermore, the $4f$ level in GdX is sufficient below the Fermi energy, the usual type of d-f or p-f mixing effect is believed to be much smaller, and thus the Ruderman-Kittel-Kasuya-Yosida (RKKY) type d-f Coulomb exchange interaction is the main part of the indirect exchange interaction between $4f$ ions (where ''d'' represents the conduction electrons, i.e., $5d$ or $6s$ electrons in rare-earth atoms, ''p'' represents the p-band holes of pnictogen).[6] Therefore, GdX are the convenient referent systems for other rare-earth monopnictides and the convenient referent systems for the Eu monochalcogenides EuX_P (X_P=O, S, Se, and Te). The studies[7–9] of magnetic properties on powder compounds of GdP, GdAs, GdSb, and GdBi suggest that they are type-II antiferromagnets below Néel temperatures T_N. However, to grow high-quality single crystal of GdX is very difficult due to the high weld point and high vapor pressure, and thus only a few studies on the electronic-transport properties of Gd monopnictides have been done in the past in a nonsystematic way. Moreover, their intrinsic electronic structure and mechanism of conductivity are still a puzzle.

In order to study the magnetic and electronic behavior of Gd monopnictides in a systematic way, recently, we have succeeded in growing large stoichiometric single crystals of GdX (X=P, As, Sb, and Bi) and nonstoichiometric single crystals of GdAs and GdP, and carefully measured the fundamental physical properties. Some magnetic properties have been reported in our recent paper.[10] In this paper, we will present the magnetoresistance, electrical resistivity, and Hall-effect measurements of these samples.

II. SAMPLE PREPARATION AND EXPERIMENT

The GdX single crystals are grown by the mineralization method (for X=P and As) and Bridgman method (for X=Sb

TABLE I. Lattice constant a, Néel temperature T_N, residual resistivity $\rho(T\rightarrow 0)$, RRR$=\rho(T=300\ \mathrm{K})/\rho(T\rightarrow 0)$, MRR$=[\rho(H=10\ \mathrm{T})-\rho(H=0)]/\rho(H=0)$, carrier concentration n, size, and the preparing method of all the GdX single crystals.

Sample	a (Å)	T_N (K)	$\rho(T\rightarrow 0)$ ($\mu\Omega$ cm)	RRR	MRR ($T=1.7$ K)	n (cm^{-3})	Size (mm^3)	Preparing method[a]
GdP	5.709	15.9	8.5	10.0	0.8		$3\times5\times5$	**M**
GdAs	5.864	18.7	5.2	16.7	8	2.1×10^{20}	$5\times6\times8$	**M**
GdSb	6.219	23.4	0.7	85.0	125[b]	4.2×10^{20}	$\phi14\times15$	**B**
GdBi	6.295	25.8	0.6	53.3	23[b]		$2\times2\times3$	**B**
ns-GdP	5.717	14.4	46	2.4	0.25		$5\times5\times5$	**M**
ns-GdAs	5.895	17.2	54	2.1	0.06		$6\times8\times8$	**M**

[a]**M**=mineralization method, **B**=Bridgman method.
[b]$T=4.2$ K.

and Bi) in tungsten crucibles. The Gd metal of 99.9% purity (turned into small flakes in a glovebox permeated with Ar gas) and P, As, Sb, and Bi metals of 99.999% purity are used. Because P and As are easy to evaporate at high temperature, a prereaction of the constituent elements is first carried out in a closed quartz ampoule at 900 °C for twelve weeks (GdP) and 550 °C for six weeks (GdAs). The polycrystalline materials of GdP and GdAs obtained by the prereaction are pressed into hard pellets at 720 °C and 1300 atm using a glass capsule method. The hard pellets are then sealed in cleared tungsten crucibles using an electron-beam gun in vacuum. For GdSb and GdBi, the starting elements of Gd and Sb or Bi are directly sealed in cleared tungsten crucibles. The crucibles are slowly heated to above 2500 °C, using a high-frequency induction furnace and kept at this temperature for 72 h for GdP and GdAs, and 2 h for GdSb and GdBi. Finally, the crucibles are drawn slowly at the rate of 1.5 mm per hour. In this way, we obtained the stoichiometric and nonstoichiometric single crystals GdP, GdAs, GdSb, and GdBi, with the dimensions shown in Table I. For all the samples, the x-ray-diffraction patterns show a single phase with NaCl structure. The room-temperature lattice constants a of these samples are also listed in Table I. The atomic ratios between Gd and pnictogen determined by chemical analysis are $1{:}0.95\pm0.01$ for the nonstoichiometric GdAs (hereafter noted as ns-GdAs), $1{:}0.96\pm0.01$ for the nonstoichiometric GdP (hereafter noted as ns-GdP), and $1{:}1.00\pm0.01$ for the four stoichiometric samples (hereafter noted as GdX with $X=$P, As, Sb, and Bi).

The samples used for our experiments are cleaved from the large single crystals. The electrical resistivity and magnetoresistance are measured by the standard four-probe method. Instead, for Hall-coefficient measurements, a four-contact geometry is used with the two voltage contacts perpendicular to the current. The magnetic field for Hall effect and magnetoresistance measurements is provided by a superconducting magnet that enabled fields up to 10 T. The temperature is obtained by an Au(0.07%-Fe)-Ag thermocouple in the electrical resistivity, magnetoresistance, and Hall-effect measurements.

III. EXPERIMENTAL RESULTS

A. Stoichiometric samples

1. Magnetoresistance

Temperature and field dependences of the magnetoresistance were measured in the transverse configuration with the current $\mathbf{I}\|[100]$ and the field $\mathbf{H}\|[010]$. The magnetic-field dependences of the transverse magnetoresistance measured at fixed T are shown in Figs. 1(a)–1(d) for the stoichiometric samples GdP, GdAs, GdSb, and GdBi, respectively. The insets in these figures show the plots of $[\rho(H)-\rho(0)]/\rho(0)$ vs H^2 for the corresponding samples. At low temperature, the transverse magnetoresistance increases with H in the investigated field range and follows approximately a $\rho(H)\propto H^2$ law for all the four samples. The large positive rations of $[\rho(H)-\rho(0)]/\rho(0)$, about 0.8, 8, 125, and 23 measured at 1.7 K (GdP, GdAs) and 4.2 K (GdSb, GdBi), are observed at 10 T for GdP, GdAs, GdSb, and GdBi, respectively (see Table I). This indicates that the stoichiometric samples GdP, GdAs, GdSb, and GdBi are the good compensated semimetallic crystals of high-quality single, which are appropriate for the de Haas–van Alphen (dHvA) effect measurements. In fact, the clear dHvA oscillations have been observed for our stoichiometric GdAs and GdSb samples at low temperature and high applied field.[11]

$\rho(T,H)$ is also measured as a function of T at fixed H for these samples. For instance, Figs. 2 and 3 illustrate the results of stoichiometric GdAs and GdSb. These data can be used to calculate the carrier concentration and the mobilities of electrons and holes as explained in Sec. IV.

2. Electrical resistivity

The electrical resistivity $\rho(T)$ is measured between 1.6 and 300 K for the stoichiometric GdP, GdAs, GdSb, and GdBi samples, as shown in Figs. 4 and 5. The four curves are qualitatively similar. At low temperatures, the resistivity first increases rapidly with increasing temperature, and shows a kink at the Néel temperature T_N. At higher temperatures the resistivity becomes linear in the temperature. The Néel temperatures, as determined from the derivative $\partial\rho/\partial T$, are found to be 15.9, 18.7, 23.4, and 25.8 K for GdP, GdAs, GdSb, and GdBi, respectively, in good agreement with our specific-heat measurements and magnetic-susceptibility data.[12] The values of residual resistivity $\rho(T\rightarrow 0)$ and ratio RRR$=\rho(T=300\ \mathrm{K})/\rho(T\rightarrow 0)$ are 8.5 $\mu\Omega$ cm and 10.0 for GdP, 5.2 $\mu\Omega$ cm and 16.7 for GdAs, 0.7 $\mu\Omega$ cm and 85.0 for GdSb, and 0.6 $\mu\Omega$ cm and 53.3 for GdBi. For GdP and GdAs the metal-like linear $\rho(T)$ behavior curves appears above $T_L\approx85$ and 70 K, respectively. In the temperature range between T_N and T_L, $\rho(T)$ deviates from the linear behavior. For GdSb and GdBi, however, the linear $\rho(T)$ behavior remains even when T is decreased near to T_N, i.e., $T_L\approx T_N$. Note that Kaldis, von

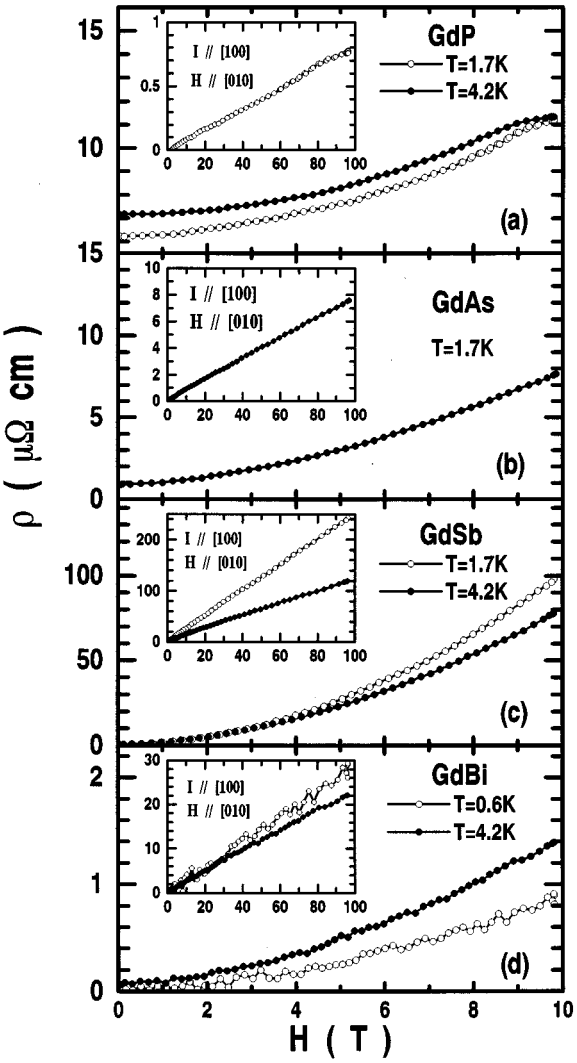

FIG. 1. Magnetic-field dependence of the transverse magnetoresistance of stoichiometric GdX. The insets {Y axis: $[\rho(H)-\rho(0)]/\rho(0)$; X axis: $H^2(T^2)$} show the plot of $[\rho(H)-\rho(0)]/\rho(0)$ vs H^2.

Schulthess, and Wachter[13] observed a sharp peak of resistivity at T_N and a negative magnetoresistance at low magnetic field for their GdP sample prepared by a high-temperature vapor growth method. In fact, a similar behavior of a negative magnetoresistance is observed only in our nonstoichiometric ns-GdP and nonstoichiometric ns-GdAs samples in the present study.[14] This negative magnetoresistance effect will be discussed in Sec. IV in detail.

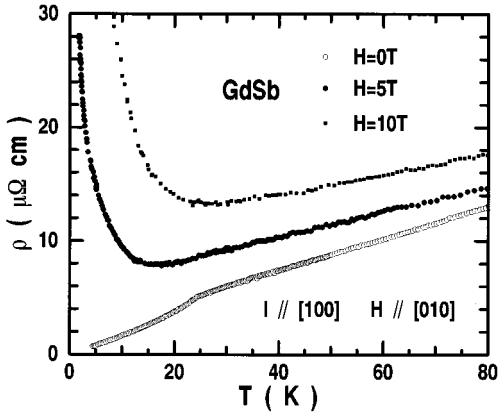

FIG. 3. Temperature dependence of the resistivity of stoichiometric GdSb measured at magnetic fields of 0, 5, and 10 T.

3. Hall effect

The Hall coefficients of GdX are measured in two ways: (1) measuring the Hall coefficient R_H as a function of H at a fixed T, and (2) measuring the Hall coefficient R_H as a function of T at a fixed H. Both measurements are carried out with $\mathbf{I}\|[100]$ and $\mathbf{H}\|[010]$. Figure 6 shows the field dependence of the Hall coefficient for the stoichiometric GdAs up to 5 T measured at $T=4.2$ K. The Hall coefficient is a negative constant ($R_H=-0.8\times10^{-8}$ m^3 C^{-1}). At a fixed T, a constant Hall coefficient is also observed for the stoichiometric GdSb up to 8 T.

Figures 7(a) and 7(b) show the temperature dependences of Hall coefficient of the stoichiometric GdAs and GdSb, respectively. Below T_N, $|R_H|$ of GdSb first decreases rapidly with increasing T, after crossing zero at about 3 K, R_H changes sign from negative to positive and $|R_H|$ increases, above T_N, then, R_H goes through a broad maximum around 30 K and, finally, $|R_H|$ decreases slowly up to 100 K. At T_N, no evident peak appears. This is very different from the behavior of R_H in Ce monopnictides.[15] The similar features are

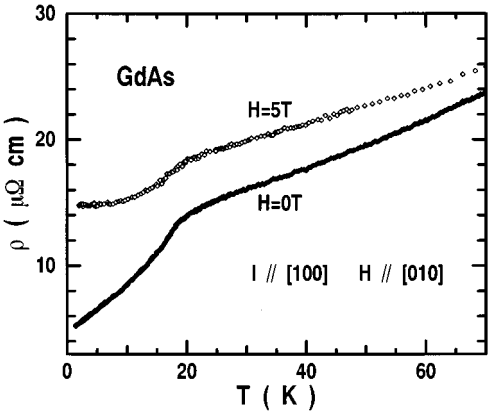

FIG. 2. Temperature dependence of the resistivity of stoichiometric GdAs measured at magnetic fields of 0 and 5 T.

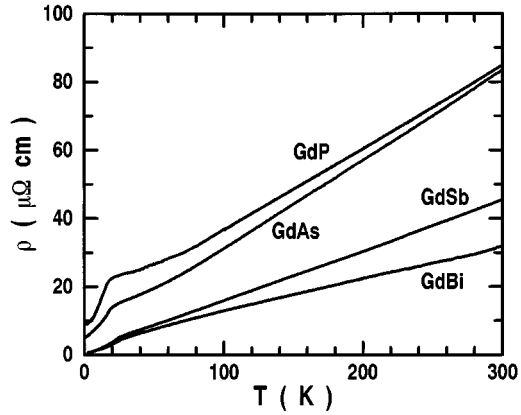

FIG. 4. Temperature dependence of the electrical resistivity of stoichiometric GdX measured at zero field.

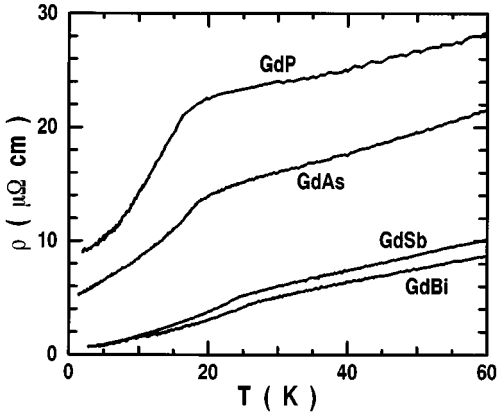

FIG. 5. Temperature dependence of the electrical resistivity of stoichiometric GdX measured at zero field and near the Néel temperature.

also observed in the stoichiometric GdAs sample in which R_H is negative up to 100 K, and a broad peak appears around 40 K. However, the R_H values are different between them, which indicates that the carrier concentrations in GdSb and GdAs are different. The measurements shown in Figs. 7(a) and 7(b) will be used to calculate the mobilities of electron and hole and the carrier concentrations in Sec. IV.

B. Nonstoichiometric samples

The Gd monopnictides GdX are typical ''exchange dominating'' systems similar to the Eu chalcogenides EuX_P. Their magnetic and transport properties are strongly dependent on the deviation of stoichiometry of the sample. For the nonstoichiometric EuX_P, there are many experimental and theoretical reports on the anomalous physical properties.[16–18] Similar anomalies are considered to exist also in the nonstoichiometric GdX. However, there is no systematical study on them so far due to the difficulty of preparing GdX single crystals. Recently, the growth of large nonstoichiometric GdX single crystals has permitted the accurate measurements of the magnetic and transport properties for them.

Figure 8 shows the field dependence of the transverse magnetoresistance for the nonstoichiometric ns-GdAs (Gd:As=1:0.95) and ns-GdP (Gd:P=1:0.96). For ns-GdAs,

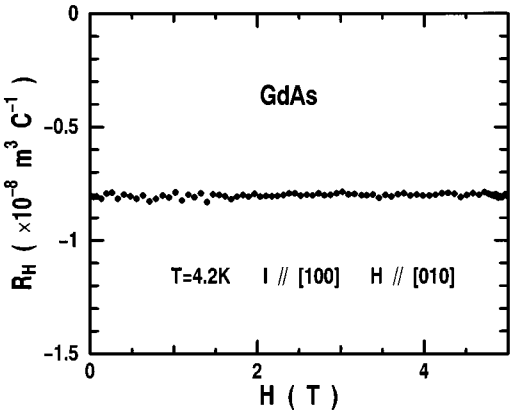

FIG. 6. Magnetic-field dependence of the Hall coefficient for stoichiometric GdAs measured at $T=4.2$ K.

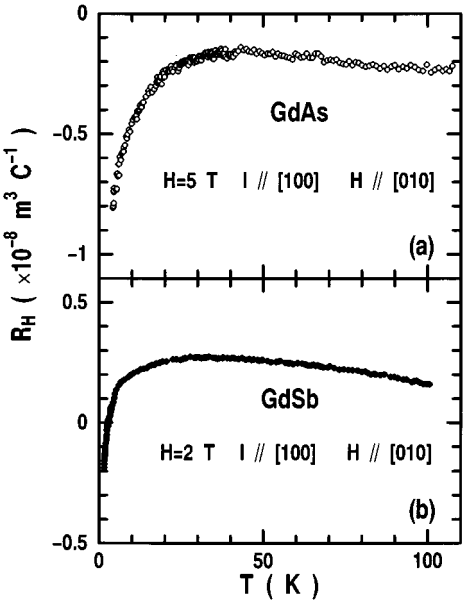

FIG. 7. Temperature dependence of the Hall coefficient for stoichiometric GdAs and GdSb measured at $H=5$ and 2 T, respectively.

the ρ-H curves measured at 1.6 and 4.2 K can be divided into four different regions, corresponding to four field ranges. In the first region ($0<H<0.5$ T), ρ decreases very rapidly with increasing H. The decrease becomes even more pronounced at lower temperature. Note that in the same temperature and field region the magnetization of ns-GdAs strongly increases.[10] In the second region ($0.5<H<1$ T), although the magnetoresistance remains negative, $|\partial\rho/\partial H|$ is considerably smaller than that in the first region. Correspondingly, the magnetization in this field range also increases nonlinearly but $|\partial M/\partial H|$ is smaller than that in the field range below 0.5 T.[10] The third region ($1<H<7$ T) corresponds to

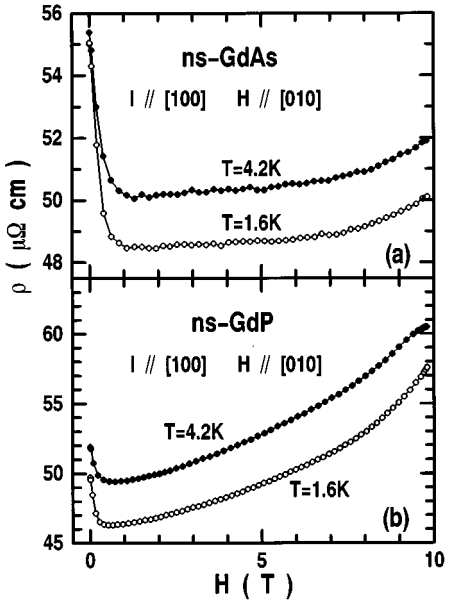

FIG. 8. Magnetic-field dependences of the transverse magnetoresistance of the nonstoichiometric ns-GdAs and ns-GdP.

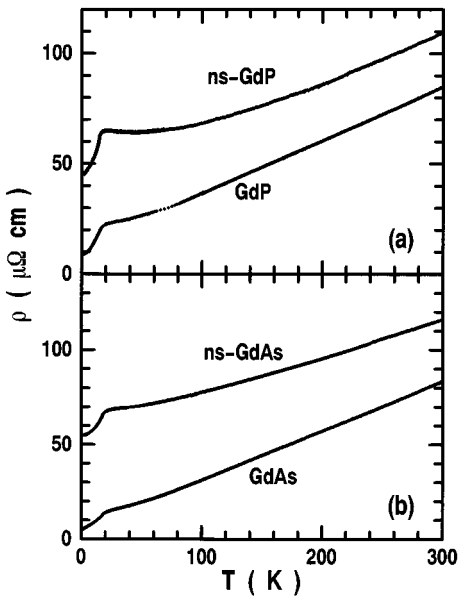

FIG. 9. Comparison between the resistivities of stoichiometric GdP (GdAs) and nonstoichiometric ns-GdP (ns-GdAs).

the canted phase. Although the differential magnetoresistance becomes positive above 1 T, $\partial\rho/\partial H$ is small and almost H independent. ρ shows a shallow minimum around 1 T. In the fourth region ($H>7$ T), although it is still in the range of the canted phase, the increase of ρ becomes more pronounced at larger fields. Similar behavior of a negative magnetoresistance at low fields is also present in the nonstoichiometric ns-GdP [Fig. 8(b)].

Figures 9(a) and 9(b) are the electrical resistivity measurements for ns-GdAs and ns-GdP, respectively. The data of the stoichiometric samples are also shown in the corresponding figures for the convenience of comparison between them. For GdAs, the two curves (of GdAs and ns-GdAs) have similar $\rho(T)$ behavior but are different in detail. As T increases, $\rho(T)$ of both GdAs and ns-GdAs first increases rapidly at lower temperatures, then goes through a kink at the Néel temperature T_N, and finally increases linearly at higher temperatures. The Néel temperatures T_N determined from the derivative $\partial\rho/\partial T$ are 18.7 K for GdAs and 17.2 K for ns-GdAs, The main differences between GdAs and ns-GdAs consist in the residual resistivity, much larger in the nonstoichiometric sample, and in the linear slope observed in the paramagnetic phase. At $T=1.6$ K, the lowest temperature of this measurement, a residual resistivity of 5.7 $\mu\Omega$ cm was found for the stoichiometric GdAs. In the nonstoichiometric ns-GdAs, however, the corresponding value is 55 $\mu\Omega$ cm, ten times larger than the value found for GdAs. Furthermore, the metal-like linear $\rho(T)$ behavior appears above $T_L=70$ K for the stoichiometric GdAs, while it appears at much higher temperatures, above $T_L=200$ K, for the nonstoichiometric ns-GdAs. Similar anomalous behaviors are also observed in ns-GdP [Fig. 9(b)]. At $T=1.6$ K, a residual resistivity of 47 $\mu\Omega$ cm was found for the nonstoichiometric ns-GdP, much larger than the corresponding value of 8.8 $\mu\Omega$ cm found for the stoichiometric GdP. While the metal-like linear $\rho(T)$ behavior appears above $T_L=200$ K for the nonstoichiometric ns-GdP, much higher than the corresponding temperature, above $T_L=85$ K, it is observed in the stoichiometric GdP. Furthermore, for the nonstoichiometric ns-GdP, a shallow minimum appears near 50 K, and a broad peak is observed around T_N instead of the kink that appeared in other GdX.

IV. DISCUSSION

A. Stoichiometric samples

1. Magnetoresistance

Transverse magnetoresistance measurements enable us to check the sample quality of a semimetal. In general, the existence of lattice defects, originating from impurities or nonstoichiometry, broadens the Landau levels. When the energy interval between the Landau levels is smaller than the level broadening, then $[\rho(H)-\rho(0)]/\rho(0)<1$ and the dHvA or Shubnikov–de Haas (SdH) signals cannot be observed.[19] For a semimetallic single crystal of high quality, in general, one observes the dHvA or SdH signals, a large value for MRR $=[\rho(H)-\rho(0)]/\rho(0)$, a large value for resistivity ratio RRR $=\rho(T=300\ \text{K})/\rho(T\rightarrow 0)$, and an approximate $\rho(H)\propto H^2$ behavior. The stoichiometric GdP, GdAs, GdSb, and GdBi samples can be considered to be the high-quality semimetallic single crystals with a good compensation between electrons and holes, because they show the large ratios of MRR and RRR (see table I), and follow an approximate $\rho(H)\propto H^2$ law at low temperature. Furthermore, clear dHvA signals have been observed for GdAs and GdSb at low temperature and high applied field.[11] Thus the experimental results obtained for these samples represent intrinsic features of pure Gd monopnictides.

2. Electrical resistivity

For the stoichiometric samples, the temperature dependence of the electrical resistivity, shown in Fig. 4, has two contributions. The first one is the normal resistivity ρ_p, caused by the electron-phonon scattering, which is linear in T at high temperatures. This is observed at the temperatures above $T_L\approx 85$, 70, 24, and 26 K for GdP, GdAs, GdSb, and GdBi, respectively. The second contribution is the magnetic part ρ_m of the resistivity. We are interested in the second part of the resistivity. The formal treatment of magnetic scattering mechanism has been carried out by Andersen and his collaborators.[20] For $T\rightarrow 0$, there are no magnon and phonon excited in the crystal and both resistivities ρ_p and ρ_m vanish. In the absence of any impurity, the conduction electrons propagate through the perfectly periodic lattice without being scattered incoherently and the resistivities ρ_p and ρ_m vanish. With increasing temperature, the conduction electrons are scattered off the thermally activated magnons and, in a ferromagnetic or antiferromagnetic metal, ρ_m contributes to the electrical resistivity together with the contributions of the electron-phonon and electron-impurity scattering. Spin wave (magnons) are the collective excitations of the aligned spins, just like phonons in the case of lattice vibrations. The electron-magnon scattering resistivity increases nonlinearly with increasing temperature. It may be the origin of the nonlinear increase of the resistivity observed in stoichiometric GdX samples below T_N (Fig. 4).

As the temperature is increased further, more and more magnetic ions can have their spin orientations affected by

thermal fluctuations. In this case, the spin-disorder scattering is usually considered to be the origin of the scattering process. In the Gd monopnictides, this spin-disorder scattering may be caused by the d-f Coulomb exchange interaction, i.e., the RKKY exchange interaction, in which the conduction $5d$ electrons interact with the f electrons, considered to be well localized.[21] Above T_N the spins of the magnetic ions become randomly oriented and the magnetic part of the resistivity, originated from the scattering between the conduction electrons and the spin disorder, saturates and becomes independent of temperature. Kasuya[22] calculated the contribution to the magnetic part of the electrical resistivity originated from this d-f scattering process for magnetic metals with magnetic ions in the S state (quenched orbital moment). Above the Néel temperature, this calculation yields a magnetic resistivity inversely proportional to the carrier concentration n. Our experimental results show that the value of $\Delta\rho=\rho(T=T_N)-\rho(T=0)\approx\rho_m$ decreases when going from GdP to GdBi (Fig. 5). For GdAs, the value of $\Delta\rho$ is about twice the value found for GdSb. This is in accord with Kasuya's theory, since our dHvA effect measurements show that the carrier concentration in GdSb is about double, as in GdAs. Thus, in stoichiometric GdX, the magnetic resistivity is considered to originate mainly from the RKKY interaction between the conduction $5d$ electrons and the $4f$ electrons. On the other hand, the critical scattering due to the short-range order is also important and affects the resistivity near the Néel temperature.[23] The fact that the warping of the $\rho(T)\sim T$ curve begins at a temperature slightly above the Néel point may be attributed to the critical scattering process. When the orientations of $4f$ spins become completely disordered at $T\gg T_N$, the resistivity originated from this d-f Coulomb exchange interaction eventually saturates and becomes independent of the temperature, thus the $\rho(T)\sim T$ curves show the metal-like linear behavior.

3. Hall effect

In magnetic materials, the Hall resistivity comprehends two contributions and is often expressed as

$$\rho_H=R_0B+R_SM, \tag{1}$$

where B is the applied magnetic field, and R_0 and R_S are referred to as the normal and the anomalous Hall coefficients, respectively. The stoichiometric GdX samples are considered to be the well-compensated semimetals. Therefore, three parameters are necessary to reproduce the electrical transport measurements. These are the concentration of conduction electrons and valence holes ($n=n_e=n_h$) and the mobilities (μ_e,μ_h) of the conduction electrons and the valence holes. As a rough calculation, we can ignore the anomalous Hall effect in Eq. (1) (Ref. 24) and the field dependence of the mobilities and carrier concentration,[25] then the charge-carrier density and the mobilities of the electrons and holes of the stoichiometric GdX samples are given by measuring the zero-field resistivity $\rho(0,T)$, the transverse magnetoresistance $\rho(H,T)$, and the Hall coefficient R_H in a simple two-band model as follows:[26–28]

$$1/\rho(0,T)=ne(\mu_h+\mu_e), \tag{2}$$

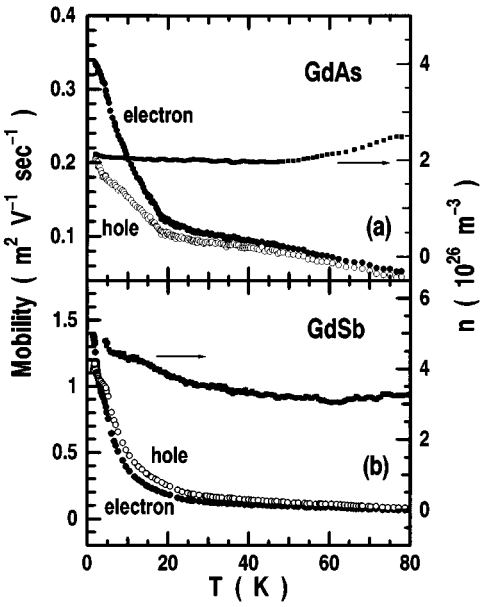

FIG. 10. Temperature dependencies of the mobilities (of electron and hole) and carrier concentration for stoichiometric GdAs and GdSb calculated with a simple two-band model.

$$R_H(H,T)=(\mu_h-\mu_e)/[ne(\mu_h+\mu_e)], \tag{3}$$

$$[\rho(H,T)-\rho(0,T)]/\rho(0,T)=\mu_h\mu_eH^2. \tag{4}$$

In Figs. 10(a) and 10(b), we show the resulting temperature dependences of the parameters n, μ_e, and μ_h for stoichiometric GdAs and GdSb, respectively.

For GdAs, the mobility of the electrons is larger than that of the holes in the investigated temperature range. This explains the measured negative Hall coefficient. Around T_N, both mobilities μ_e and μ_h show an abrupt change in agreement with the above given analysis of the magnetic scattering around T_N. Below T_N, the difference between μ_e and μ_h rapidly increases with decreasing T, and the carrier concentration n slowly increases. According to Eq. (3), the increase of n will cause a decrease of $|R_H|$, but the experiments (Fig. 7) have shown that $|R_H|$ increases still at low temperatures. Thus, the rapid increase of $|R_H|$ below T_N seems to be determined by an increase in the mobilities. Furthermore, the slopes of all three curves of μ_e, μ_h, and n [Fig. 10(a)] vary slightly near 45 K. This may be related to the broad maximum of R_H that has appeared around the same temperature. The origin of the relatively rapid increase of n and decrease of μ_e and μ_h at $T>45$ K is not known yet.

For GdSb, the important feature is $\mu_e>\mu_h$ below 3 K and $\mu_e<\mu_h$ above 3 K, which leads to the change of sign of R_H at this temperature. The faster variation of R_H at low temperatures seems to be also due almost entirely to the increase in the mobilities for the same reason as that in GdAs. It is interesting to note that the mobility difference between electrons and holes in GdSb is very small at low temperature, which is the same characteristic as in LaSb. In GdAs, however, this difference is relatively larger, this may be due to the fact that the Fermi wave vector in GdAs is smaller, thus the mixing of the p hole in conduction band is weaker, and

magnetic scattering or phonon scattering causes the larger mobility for the conduction-band electrons. It is also interesting to notice that using Eqs. (2)–(4) a similar calculation has been made for stoichiometric YbAs by Oyamada *et al.*[29] The results confirm that the mobility of holes in YbAs does not increase below 80 K, while the mobility of electrons increases strongly. This indicates that at low temperatures, in YbAs, the resistivity is mainly determined by the mobility of the electrons. However, our results for stoichiometric GdAs [Fig. 10(a)] show that the mobility of the holes clearly increases below T_N, though it is always lower than the mobility of the electrons. Furthermore, for GdSb, we obtained nearly equal mobilities of holes and electrons [Fig. 10(b)]. Thus, even at low temperatures, the contribution of the holes to resistivity cannot be ignored in GdX. However, for different RX system, one should normally expect different electron and hole mobilities, as a consequence of the difference in the $4f$ level, the CEF splitting, and the electronic structure.

At 4.2 K, we find a free-carrier concentration of $n=\mu_e=\mu_h=2.07\times10^{20}$ cm^{-3}=0.010(4) per Gd atom for GdAs, this value is larger than the carrier number of 0.0024 per La atom in LaAs and is smaller than the carrier number of 0.014 per Yb atom in YbAs. Recently, we could observe clear dHvA signals for GdAs. The carrier number determined from the dHvA effect measurements is 0.011 per Gd atom that is consistent with the Hall-effect measurements. For GdSb, the carrier number determined from our Hall-effect measurements is $n=\mu_e=\mu_h=4.2\times10^{20}$ cm^{-3} =0.025(2) per Gd atom at 4.2 K, this value is also larger than $n=0.014(5)$ per La atom in LaSb and smaller than $n=0.026(2)$ per Tm atom in TmSb (single crystal of YbSb has not been grown so far) and is consistent with the dHvA measurements, which gives $n=0.024(5)$ per Gd atom.[30]

B. Nonstoichiometric samples: The trapped magnetic polaron effects

It is well known that the average Coulomb potential (P.E.) and the average kinetic energy (K.E.) of one electron in an electron system approximate to $e^2/(r_s a_H)$ and $m^{-1}(\hbar/r_s a_H)^2$, respectively. Thus, as an estimate in order of magnitude, there is

$$\frac{\text{P.E.}}{\text{K.E.}}=r_S, \tag{5}$$

here, $a_H=\hbar^2/(me^2)$ is the Bohr radius, r_s is a parameter without a unit used to judge the electron concentration, and $\frac{4}{3}\pi(r_s a_H)^3$ represents the average volume of an electron sphere.

In the high electron concentration limit, $r_s \ll 1$, the Fermi kinetic energy of an electron is more important than the Coulomb potential. Thus it is an extended state electron, and can move through the lattice. Such an electron system is called the electron gas. On the contrary, in low electron concentration limit, $r_s \gg 1$, according to Eq. (5), the Coulomb interaction between electrons overcomes the kinetic energy, thus the system does not exhibit the feature of Fermi electron gas. Such a system (Coulomb-correlation energy is larger than the electron's kinetic energy) is called strongly correlated electron system. Wigner[31] first pointed out that in low carrier limit the strong correlation effect can localize the electrons to form the electron lattice, which is called Wigner lattice. Since electron's Fermi kinetic energy is in proportion to r_s^{-2}, and the Coulomb correlated energy is in proportion to r_s^{-1}, evidently in a strongly correlated electron system, if the electron concentration is low enough, the formation of Wigner lattice is more favorable energetically.

However, so far, no real Wigner crystal has been observed except a two-dimensional one on the surface of He^{II}. This is partly because the crystal has a large zero-point vibration and thus the Wigner crystal is very easily melted into the liquid phase and partly because even a very small amount of impurity changes it to the impurity localized state.[15] Furthermore, in low carrier magnetic system with some defects, the carriers are more easily localized in the defects, and due to the existence of magnetic exchange interaction, so-called trapped magnetic polarons around the localized carriers are expected to be formed instead of the Wigner lattice. In fact, the clear trapped magnetic polaron effects have been observed in nonstoichiometric semiconductor EuTe (Refs. 16 and 17) and other Eu chalcogenides[18] with very low carrier concentrations ($<10^{19}$ cm^{-3}), and some theoretically studies[32] have been carried out for this series. Gd monopnictides GdX are also the ''exchange dominating'' systems similar to Eu chalcogenides EuX_P as described in the introduction. However, our Hall effect and dHvA effect measurements show that the carrier concentrations in GdX are much larger than that in EuX_P. Then, the questions one may ask are if the trapped magnetic polaron state could also be formed in semimetallic GdX? If it exists, what are the differences in the origin of formation of trapped magnetic polarons between GdX and EuX_P? In our recent experiments, the anomalous magnetic and transport properties have been found for the Gd-rich nonstoichiometric GdX, which can be considered to be the evidences of formation of trapped magnetic polaron states in nonstoichiometric Gd monopnictides. On the basis of the trapped magnetic polaron model, the anomalous magnetic behaviors of Gd-rich GdX have been explained in our recent paper.[10] In the following, we will discuss the trapped magnetic polaron effects on the transport properties of the nonstoichiometric GdX.

The formation of the trapped magnetic polarons in nonstoichiometric Gd monopnictides has already been described in our recent short communication.[15] The basic idea is the following. In considering the state of a conduction electron in an antiferromagnetic crystal, it is customary to assume that it does not disturb the magnetic ordering of the crystal. In some cases, however (for example, in low carrier systems), an energetically more favorable state is achieved when the electrons become localized and interact with the surrounding magnetic ions.[33] In the nonstoichiometric GdX samples, some electrons, originating from the X vacancies, are trapped by the Coulomb potential of the X vacancies. The strong d-f exchange interaction between the trapped electrons and the neighboring $4f$ spins aligns the $4f$ spins. A trapped electron generates a region with ferromagnetic ordered $4f$ spins around itself and a trapped magnetic polaron is formed. When the X vacancies move through the crystal, the trapped magnetic polarons automatically also move.

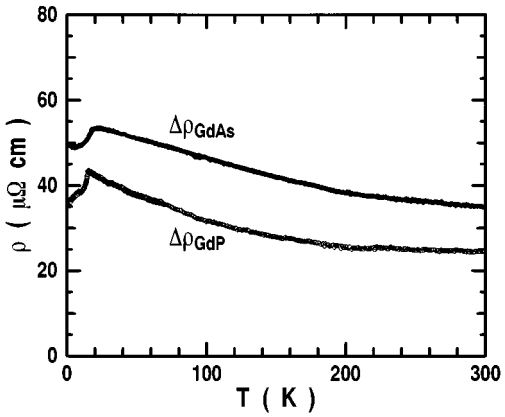

FIG. 11. Temperature dependence of the resistivity difference between nonstoichiometric ns-GdP (ns-GdAs) and stoichiometric GdP (GdAs).

According to the trapped magnetic polaron model, the anomalous magnetoresistance behavior observed in nonstoichiometric Gd monopnictides, as an example in ns-GdAs, can be explained as following: At zero field the trapped magnetic polarons have randomly oriented moments, yielding a large contribution to the resistivity through the electron-polaron scattering. With increasing temperature, the d-f exchange interaction within the polarons becomes gradually weakened by thermal fluctuation. This explains why below 0.5 T $|d\rho/dH|$ is smaller at 4.2 than at 1.6 K. Similarly, with increasing field, the moments of polarons, canted in low field, are rapidly aligned to the ferromagnetic configuration. Thus, a pronounced drop appears in the resistivity with increasing field in the low-field region. As the field is raised further, the effect of magnetic polaron on the resistivity becomes smaller, and gradually the intrinsic positive magnetoresistance of the semimetal becomes dominant. At high enough fields (above 7 T), the scattering off the trapped magnetic polaron mechanism is not expected, and the magnetoresistance of ns-GdAs approximately follows a $\rho(H)\propto H^2$ law, similar to the stoichiometric GdAs sample.

In the nonstoichiometric ns-GdAs and ns-GdP, a nonlinear $\rho(T)$ behavior was observed up to 200 K. Because the difference of the Néel temperatures between stoichiometric and nonstoichiometric samples are very small (about 1.5 K for both GdAs and GdP), and the critical scattering is important only near the Néel temperature, it is natural to believe that the critical scattering vanishes near 70 K in ns-GdAs and near 85 K in ns-GdP, as it does in GdAs and GdP, when the resistivity observed for the stoichiometric samples becomes linear in temperature. The origin of the nonlinear resistivity between T_N and T_L in the nonstoichiometric sample is therefore thought to be not only due to the critical scattering, but also due to another additional scattering process. We interpret this anomaly as an indication of the formation of trapped magnetic polarons. For the conduction electrons, the formation of trapped magnetic polarons in nonstoichiometric GdX results in an additional scattering, superimposed on the intrinsic scattering of pure GdX. This leads to the large residual resistivity, the large change of $d\rho/dT$ around T_N, and the nonlinear $\rho-T$ behavior up to higher temperatures.

Figure 11 shows the resistivity difference between stoichiometric and nonstoichiometric samples for both GdAs and GdP. Above 200 K, the values of resistivity difference are smaller and approach to constants. Thus, the trapped magnetic polaron states formed in ns-GdAs and ns-GdP are considered to be disintegrated above 200 K, which is in accord with our susceptibility measurements.[34] Further evidence of the formation of trapped magnetic polaron states in the nonstoichiometric Gd monopnictides are the nonlinear magnetization in low fields, the lager susceptibility at low temperatures, and the smaller entropy near Néel point, etc.[10,14,34]

It is well known that the trapped magnetic polaron effects are evident only in some low carrier systems, i.e., in some strongly correlated electron systems as described above. Although the trapped magnetic polaron effects have been found in nonstoichiometric semiconductors as EuTe (Refs. 16 and 17) and other Eu chalcogenides[18] with very low carrier concentrations, for semimetals, however, the effects of trapped magnetic polarons are observed for the first time in our recent experiments. In contrast to the Eu chalcogenides, the usual type of d-f mixing can be ignored in GdX, because the $4f$ level is deep and an additional RKKY interaction becomes important as discussed in Ref. 35. The carrier concentrations in GdX ($\sim 10^{20}$–10^{21} cm^{-3}) are much larger than that in semiconductors Eu chalcogenides ($\sim 10^{19}$ cm^{-3}). Furthermore, because of the different electron spin configurations, the He-like model with singlet or triplet spin configurations of impurity electrons used for EuTe (Ref. 32) is no longer valid for Gd monopnictides. Thus, in order to acquire a deep understanding of the formation of trapped magnetic polaron states in nonstoichiometric Gd monopnictides, further experimental and theoretical studies are necessary.

V. CONCLUSION

The transport properties of Gd monopnictides GdX both stoichiometric single crystals (X=P, As, Sb, and Bi) and nonstoichiometric single crystals (X=P and As) have been investigated by measuring their resistivity, magnetoresistance, and Hall effect. Stoichiometric GdX behaves as expected for the well-compensated semimetals that order antiferromagnetically at T_N=15.9 K for GdP, 18.7 K for GdAs, 23.4 K for GdSb, and 25.8 K for GdBi. Their transverse magnetoresistance measured at low temperature follows a $\rho(H)\propto H^2$ law, and the larger positive ratios $[\rho(H)-\rho(0)]/\rho(0)$ are observed at H=10 T. The temperature dependence of the resistivity can be explained by the d-f Coulomb scattering at lower temperatures. A calculation based on a simple two-band model yields that the observed rapid change of the Hall coefficient R_H below T_N is due to the increasing mobilities of the conduction electrons and valence holes. At 4.2 K, the carrier concentration determined from the Hall-effect measurements is 0.010(4) per Gd atom for GdAs and 0.025(2) per Gd atom for GdSb, which are in a good agreement with the dHvA measurements. The scattering mechanisms appearing in stoichiometric GdX are considered to appear also in nonstoichiometric GdX. But, comparing with the stoichiometric samples, the nonstoichiometric samples ns-GdAs and ns-GdP show some anomalies in the transport properties such as a large negative magnetoresistance at low

temperature and low magnetic field, and a nonlinear resistivity at higher temperatures. These anomalies can be qualitatively understood within the framework of the trapped magnetic polaron model.

ACKNOWLEDGMENT

We would like to thank Dr. M. Umehara for helpful discussion.

*Present address: The Oarai Branch, Institute for Materials Research, Tohoku University, Oarai, Ibaraki, 311-13 Japan.

[1] T. Suzuki, Jpn. J. Appl. Phys. Series **8**, 267 (1993).

[2] T. Suzuki, Physica B **186&188**, 347 (1993).

[3] T. Kasuya, T. Suzuki, and Y. Haga, J. Phys. Soc. Jpn. **62**, 2549 (1993).

[4] A. Hasegawa and A. Yanase, J. Phys. Soc. Jpn. **42**, 492 (1977).

[5] T. Kasuya, O. Sakai, J. Tanaka, H. Kitazawa, and T. Suzuki, J. Magn. Magn. Mater. **63&64**, 9 (1987).

[6] T. Kusuya, J. Alloys Compounds **192**, 11 (1993).

[7] N. Nereson and V. Struebing, in *Magnetism and Magnetic Materials*, Proceedings of the 17th Annual Conference on Magnetism and Magnetic Materials, edited by C. D. Graham, Jr. and J. J. Rhyne, AIP Conf. Proc. No. 5 (AIP, New York, 1972), p. 1385.

[8] T. R. McGuire, R. J. Gambina, S. J. Pickart, and H. A. Alperin, J. Appl. Phys. **40**, 1009 (1969).

[9] F. Hulliger, in *Handbook on the Physics and Chemistry of Rare Earths*, edited by K. A. Gschneidner, Jr. and L. R. Eyring (North-Holland, Amsterdam, 1979), Vol. 4, p. 191.

[10] D. X. Li, Y. Haga, H. Shida, T. Suzuki, T. Koide, and G. Kido, Phys. Rev. B **53**, 8473 (1996).

[11] R. Settai, Dr. thesis, Tohoku University, 1993.

[12] D. X. Li, Y. Haga, H. Shida, and T. Suzuki (unpublished).

[13] E. Kaldis, G. von Schulthess, and P. Wachter, Solid State Commun. **17**, 1401 (1975).

[14] D. X. Li, Y. Haga, H. Shida, and T. Suzuki, Solid State Commun. **93**, 1165 (1995).

[15] T. Kasuya, Y. Haga, Y. S. Kwon, and T. Suzuki, Physica B **186&188**, 9 (1993).

[16] Y. Shapira, S. Foner, N. F. Oliveira, Jr., and T. B. Reed, Phys. Rev. B **5**, 2647 (1972).

[17] N. F. Oliveira, Jr., S. Foner, Y. Shapira, and T. B. Reed, Phys. Rev. B **5**, 2634 (1972).

[18] S. von Molner and S. Methfessel, J. Appl. Phys. **38**, 959 (1967).

[19] C. Kittle, in *Introduction to Solid State Physics*, Sixth ed., edited by R. McConnin (Wiley, New York, 1986).

[20] N. H. Andersen and H. Smith, Phys. Rev. B **19**, 384 (1979).

[21] A. Narita and T. Kasuya, J. Magn. Magn. Mater. **52**, 373 (1985).

[22] T. Kasuya, Prog. Theor. Phys. **16**, 58 (1956).

[23] T. G. Richard and D. J. W. Geldart, Phys. Rev. B **15**, 1502 (1977).

[24] This is guided by the following two facts: One is that from Eq. (1) if the magnetization is nonlinear and R_S is sufficiently large, the $R_H - H$ curve would also display the nonlinear feature. For ns-GdAs, although the clear nonlinear magnetization was observed at low fields, a constant Hall coefficient R_H is also observed in the same field range (Ref. 10). Another fact is that the measurements of field dependence of Hall coefficient show a constant R_H value for pure GdAs and GdSb. Thus, as a rough calculation, it is assumed that $R_S M \ll R_0 B$ and $R_H \approx R_0$ for all GdX at all temperatures and magnetic fields. In fact, the normal Hall coefficient is generally much larger than the anomalous Hall coefficient in low carrier systems. Gd monopnictides just are the typical low carrier systems.

[25] A. Oyamada, C. Ayache, T. Suzuki, J. Rossat-Mignod, and T. Kasuya, J. Magn. Magn. Mater. **90&91**, 443 (1990).

[26] S. Minomura, G. Fujii, O. Shimomura, H. Nagano, and S. Tanuma, *Proceedings of the 12th Low Temperature Physics Conference, Kyoto*, 1970 (Keigaku, Tokyo, 1971).

[27] D. Jérome and M. Rieux, Solid State Commun. **7**, 957 (1969).

[28] H. Nozaki, H. Wada, and S. Takekawa, J. Phys. Soc. Jpn. **60**, 3510 (1991).

[29] A. Oyamada, C. Ayache, T. Suzuki, J. Rossat-Mignod, and T. Kasuya, J. Magn. Magn. Mater. **90&91**, 443 (1990).

[30] R. Settai, T. Goto, S. Sakatsume, Y. S. Kwon, T. Suzuki, Y. Kaneta, and O. Sakai, J. Phys. Soc. Jpn. **63**, 3026 (1994).

[31] E. P. Wigner, Phys. Rev. **46**, 1002 (1934). E. P. Wigner, Trans. Faraday Society **34**, 678 (1938).

[32] For example, M. Umehara, Phys. Rev. B **46**, 12 323 (1992).

[33] E. L. Nagaev, JETP Lett. **6**, 18 (1967).

[34] D. X. Li, Y. Haga, H. Shida, and T. Suzuki, Solid State Commun. **98**, 513 (1996).

[35] P. Wachter and E. Kaldis, Solid State Commun. **34**, 241 (1980).